

Numerical investigation on temperature-dependence of luminous properties of blue/violet LEDs

ZHANG LINGKUN, WANG DANGHUI*, CHE YUANG, ZHANG MENG FAN, YUAN TIANHAO

College of New Energy of Xi'an Shiyou University, Xi'an 710065, China

In recent years, the short-wavelength blue/ultraviolet LED has attracted great attention in the fields of pathogen killing, full-color display, near-field communication, high-density optical storage and so on. In this study, the relationships between bandgap, luminescence properties, electrical properties and temperature of III-nitride multiple quantum wells violet LED and blue LED are investigated using APSYS software. The conclusions indicate that the bandgap, spontaneous emission spectrum, optical output power, internal quantum efficiency and ideality factor are strongly temperature-dependent in the studied temperature range. Further, temperature has a greater impact on the luminescence properties and electrical properties of blue LEDs than those of violet LEDs. This paper elucidates the effect of temperature on the luminous efficiency of III-nitride blue/violet LEDs at the examined temperatures, which provides theoretical support for further improving and optimizing the quantum efficiency and luminous properties of blue/violet LEDs.

(Received January 11, 2024; accepted July 30, 2024)

Keywords: Blue/violet light-emitting diode, Temperature-dependence, Quantum efficiency, Electrical properties

1. Introduction

In the past few decades, III-nitride and their compounds have become key candidates for the fabrication of optoelectronic, such as light-emitting diodes (LEDs), laser diodes (LDs) and infrared detectors due to the excellent electrical properties, luminescence properties and continuously adjustable bandgap between 0.7 and 6.2 eV [1-4]. Blue/green, blue/violet and ultraviolet light LEDs based on solid-state lighting technology have the advantages of longer lifetime, lower power consumption and higher luminous efficiency and become the ideal light sources. However, the luminous efficiency of short wavelength LEDs is primarily hindered by some issues such as carrier injection efficiency, carrier leakage, and heat dissipation within the active region of the multiple quantum wells (MQWs) [5-7].

To improve the quantum efficiency, in particularly external quantum efficiency (EQE) of blue/violet LEDs in the case of higher current density injection, researchers have utilized AlGa_{0.944}N as an electron-blocking layer (EBL) to reduce carrier leakage in MQWs. Additionally, approaches such as adjusting the potential/barrier parameters of the last barrier in the MQWs [8], implementing superlattice, and content chirp structure to enhance LED quantum efficiency [9]. Temperature, as one of the key factors affecting quantum efficiency. Temperature, as one of the key factors affecting quantum efficiency, has a great influence on the spontaneous polarization effect and piezoelectric polarization effect existing in the wurtzite crystal lattice, as well as the strain-field remaining in the active region. As well known, the increasing temperature also exacerbates the influence of the quantum-confined Stark effect (QCSE) on the luminous efficiency for the polar LEDs [10] and resulting a redshift of the radiative peak wavelength and a

subsequent decreasing in luminous efficiency. Therefore, it is of great significance to deeply explore the impact mechanisms of temperature-dependent to improve luminous efficiency of the short wavelength LEDs.

In this study, the relationships between bandgap, luminescence properties, electrical properties and temperature of III-nitride multi-quantum well blue/violet LEDs are investigated using APSYS software. The bandgap, spontaneous emission spectrum, optical output power, internal quantum efficiency and ideality factor of the violet LED are compared with the blue LED under the studied temperatures.

2. Models of LEDs

The model of blue/violet LEDs are illustrated in Fig. 1. Fig. 1(a) presents the schematic of an AlGa_{0.944}N-based violet LED, which grows along the *c*-axis and the dimensions of 350 μm x 350 μm, and comprises a sapphire substrate (100 μm thickness), an n-AlGa_{0.944}N layer (4 μm thickness, doping concentration of $5 \times 10^{18} \text{ cm}^{-3}$), and 5 pairs of MQWs (12 nm Al_{0.056}Ga_{0.944}N/3 nm GaN). Following as a p-Al_{0.12}Ga_{0.88}N electron barrier layer (20 nm thickness), a p-Al_{0.056}Ga_{0.944}N layer (doping concentration of $2 \times 10^{19} \text{ cm}^{-3}$, 100 nm thickness), and a p-GaN ohmic contact layer (100 nm thickness). The selected temperature range is from 255 K to 375 K with a step temperature of 40K. In Fig. 1(b), the schematic of an InGa_{0.9}N-based blue LED, which consists of a sapphire substrate (100 μm thickness), an n-In_{0.1}Ga_{0.9}N layer (4 μm thickness, doping concentration of $5 \times 10^{18} \text{ cm}^{-3}$), and 5 pairs of quantum wells (3 nm In_{0.1}Ga_{0.9}N/12 nm GaN). Furthermore, it incorporates a p-In_{0.2}Ga_{0.8}N electron barrier layer (20 nm thickness, doping concentration of $2 \times 10^{19} \text{ cm}^{-3}$), a p-In_{0.15}Ga_{0.85}N layer (20 nm thickness), and a

p-GaN ohmic contact layer (100 nm thickness).

3. Results and discussions

3.1. Bandgap diagram

Fig. 2 depicts the relationships between bandgap diagram and temperature of violet LED and blue LED. As illustrated in Fig. 2(a), there is subtle changes in the potential barrier within MQWs of the violet LED when the temperature increases from 255 K to 295 K. Consequently, the Fermi level of the valence band and the potential well height is weakly affected, which resulting in a negligible impact on hole injection efficiency with the increasing

temperature, and indicating that temperature has little effect on the radiative recombination probability between electrons and holes within the active region. In Fig. 2(b), one can see that there is a small change in the potential barrier within MQWs of the blue LED when the temperature increases from 255 K to 295 K. However, as the temperature increases to 375 K, the bandgap bending and tilt obviously occurred in the MQWs, which is due to the reducing the spatial overlaps of electron and hole wave functions, consequently diminishing the probability of radiation recombination and luminous efficiency [11]. Therefore, it can be concluded that temperature has a more sensitive effect on the radiative recombination in the active region of blue LED compared with violet LED.

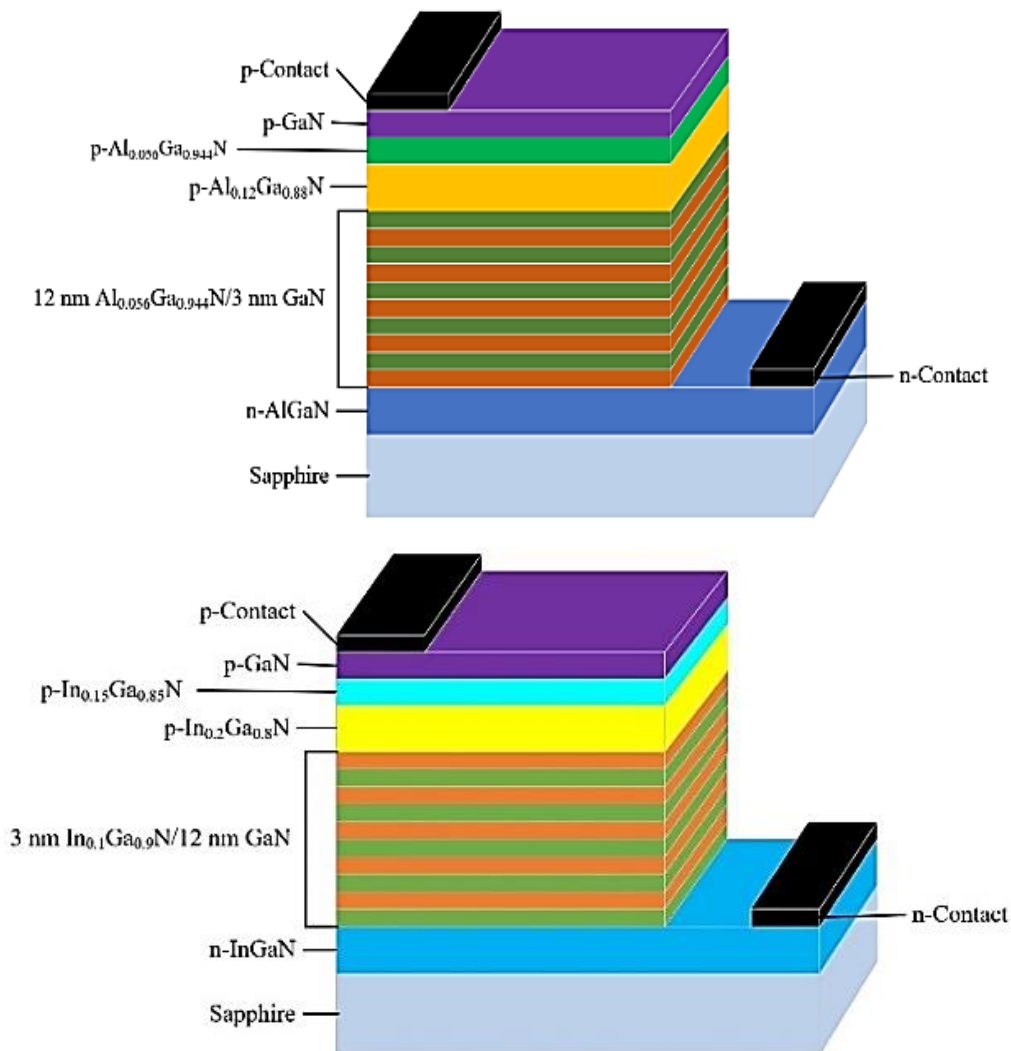


Fig. 1. Structure diagram of LEDs (a) Violet LED; (b) Blue LED (color online)

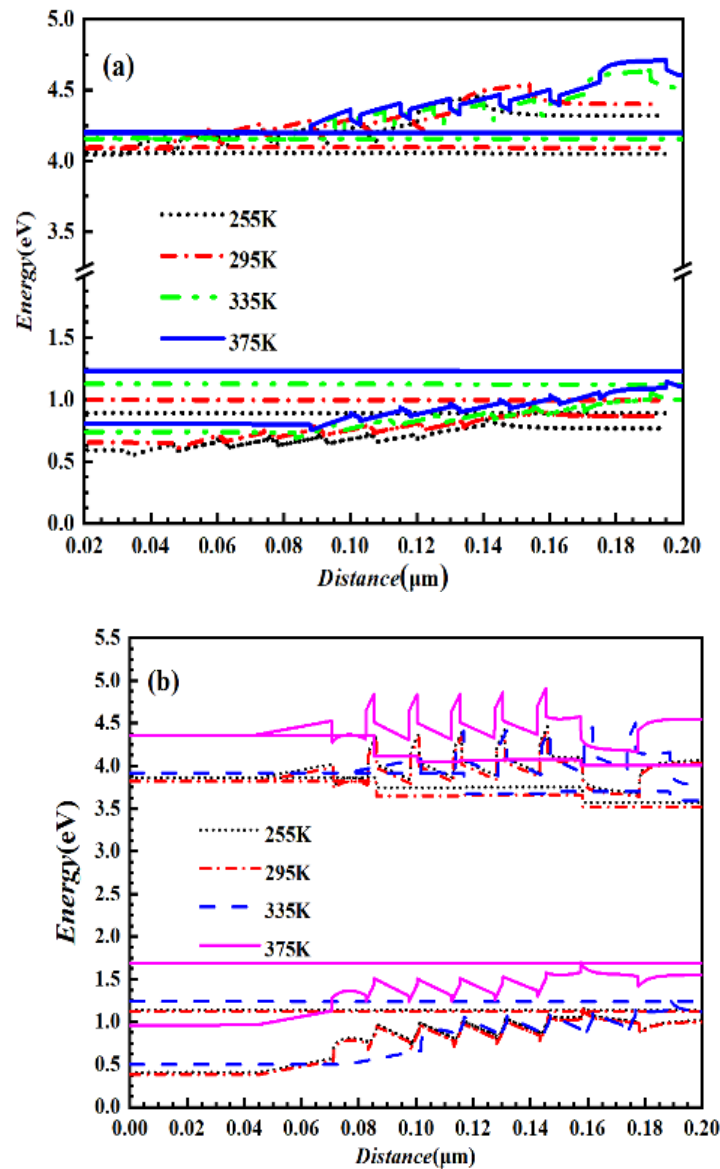


Fig. 2. Bandgaps diagram of the MQW LEDs under the studied temperatures: (a) Violet LED; (b) Blue LED (color online)

3.2. Spontaneous emission spectrum

The spontaneous emission spectral of blue and violet LEDs are presented in Fig. 3. From Fig. 3, we can find there the peak wavelengths of violet LED and blue LED are redshifted with the increasing temperatures. The redshift of violet LED is from 3.490 eV (355.3 nm) to 3.453 eV (359.1 nm), while the redshift of blue LED is from 2.987 eV (415.2 nm) to 2.932 eV (422.9 nm) during the temperature changes from 255 K to 375 K. The calculated redshift of the peak wavelength of the violet LED is 37 meV, which is lower than that redshift of the blue LED 55 meV. In additional, Fig. 3 illuminates that with increasing temperature the intensity of the peak decrease for both violet and blue LEDs, while the full width at half maximum (FWHM) of the peak wavelengths gradually become wider (see from Table 1)

with the increasing temperatures, which indicate that a reduction in carrier lifetime with the increasing temperature, consequently resulting in decreased luminous efficiency [12].

3.3. Optical output power

The tendency of the optical output power of violet and blue LEDs with the temperatures are shown in Fig. 4. From Fig. 4(a), one can see that the optical output power increase with the increasing current density at the certain temperature, while decrease as the increasing temperature at a certain current density for both violet and blue LEDs. Further, it can also be seen that the optical output power of the violet LED exhibits a trend of saturation at a current density of 600A/m, while the optical output power of the

blue LED has an upward trend, which indicates that the luminous efficiency of the violet LED is lower than that of

the blue LED when higher current density injection [13].

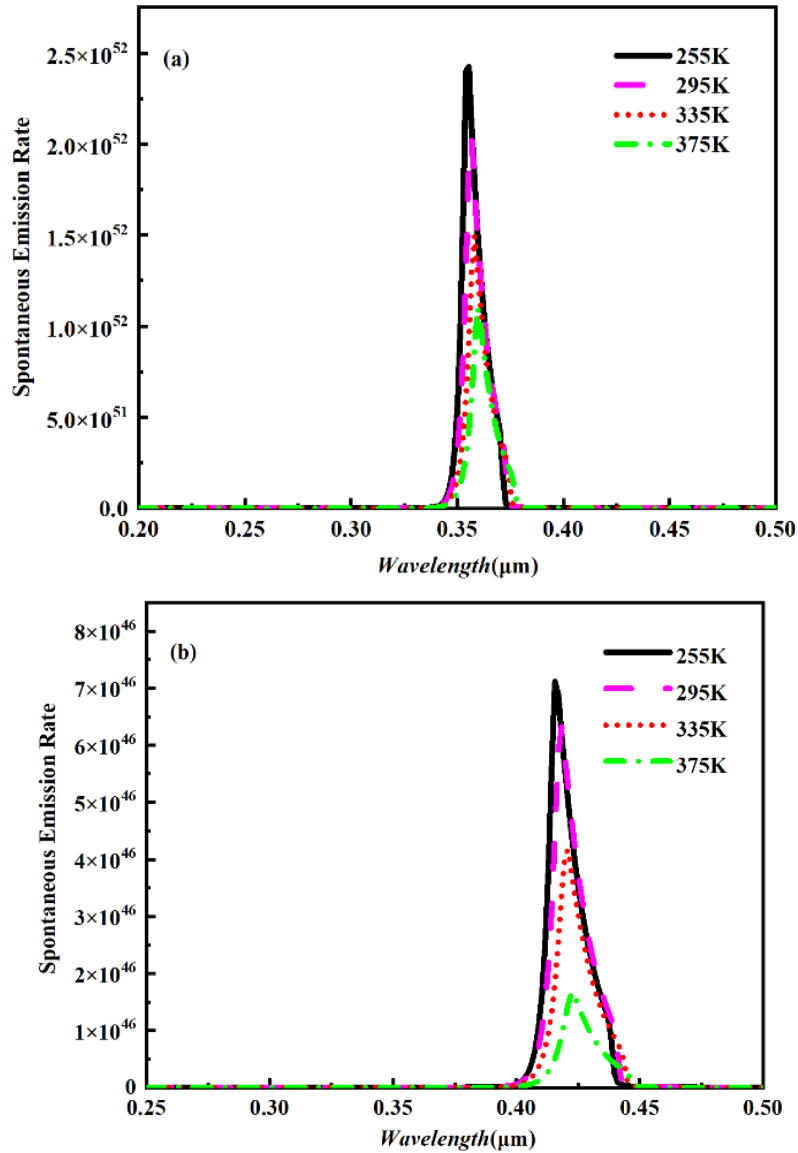


Fig. 3. Spontaneous spectral diagram of LEDs under the studied temperature: (a) Violet LED; (b) Blue LED (color online)

Table 1. FWHMs of violet LED and blue LED at studied temperatures

Temperature	255 K	295 K	335 K	375 K
Violet LED	9.2 nm (87.3meV)	9.3 nm (90.2meV)	10.3 nm (98.9meV)	12.0 nm (114.0meV)
Blue LED	11.4 nm (80.5meV)	14.2 nm (99.7meV)	14.9nm (103.6meV)	17.1 nm (117.1meV)

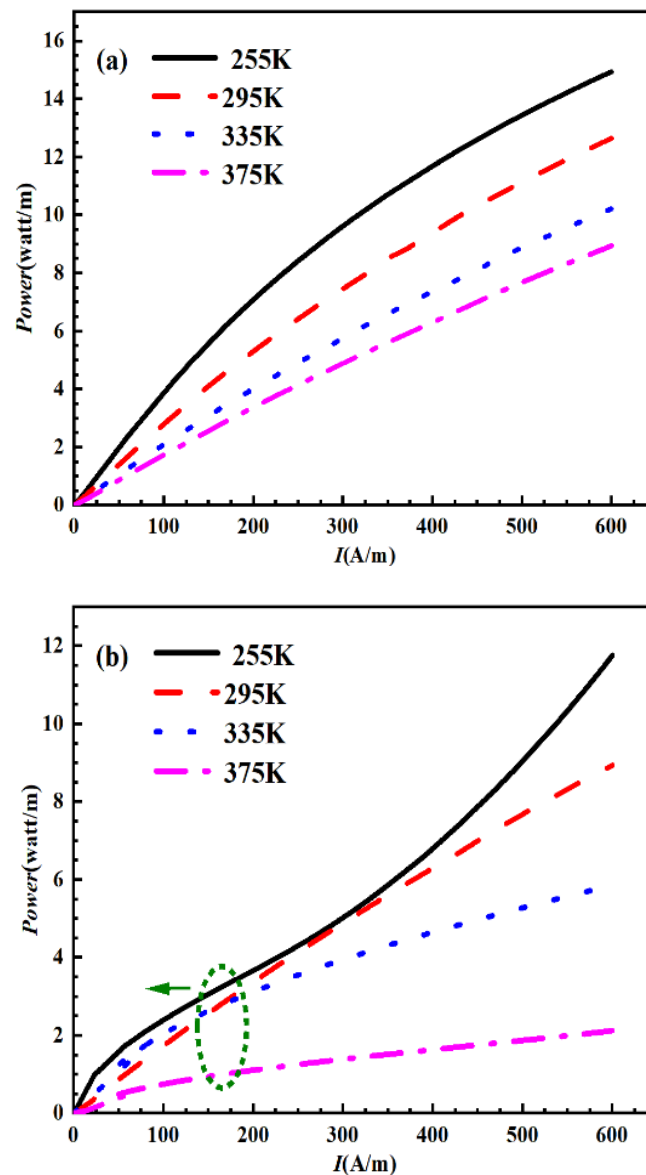


Fig. 4. The relationships between the optical output power of the LEDs under the studied temperature: (a) Violet LED; (b) Blue LED (color online)

3.4. Quantum efficiency

The quantum efficiency of the violet LED and blue LED are shown in Fig. 5. From Fig.5, quantum efficiency of violet LED and blue LEDs are shown the similar tendency of first increasing and then decreasing with the studied temperature from 255 K to 375 K, which is well known as the efficiency-droop effect [14] and primarily caused by Auger recombination, polarization effect, and carrier localization effect. The efficiency-droop factor (EDF) of LEDs can be calculated using Eq. (1) and is summarized in Table 2 [15].

$$EDF = \frac{IQE_{max} - IQE_{min}}{IQE_{max}} \quad (1)$$

One can see from Table 2, the efficiency-droop factor of the violet LED decreases from 37.65% to 0.09% with increasing temperature, while the efficiency-droop factor of the blue LED only decreases by 23.79% under the same temperature, which is attributed to the more tilted bandgap of blue LEDs than that of the violet LED and resulted in a higher barrier under the same current injection [16].

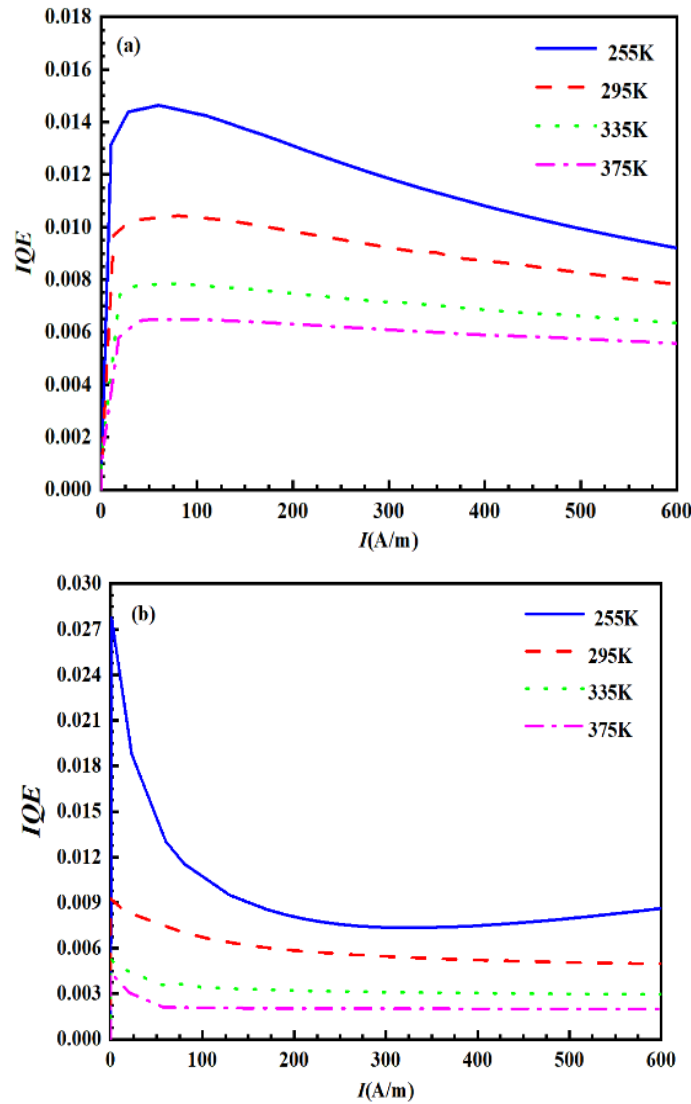


Fig. 5. Relationship between temperature and internal quantum efficiency: (a) Violet LED; (b) Blue LED (color online)

Table 2. Efficiency-droop Factor of two s at different temperatures

Temperature	255 K	295 K	335 K	375 K
Violet LED	37.65 %	25.65 %	19.47 %	0.09 %
Blue LED	68.88 %	46.64 %	44.47 %	44.43 %

3.5. Bandgaps

The temperature-dependence of the bandgap of semiconductor materials is widely recognized following Varshni's empirical formula [17], as expressed in Eq. (2):

$$E_g(T) = E_g(0) - \frac{\alpha T^2}{T + \beta} \quad (2)$$

Here, $E_g(0)$ is the bandgap at 0K, α and β are the temperature coefficients of bandgap, respectively. The coefficients of α and β for InN, GaN, and AlN are listed

in Table 3.

For $\text{Al}_x\text{Ga}_{1-x}\text{N}/\text{GaN}$ violet LEDs, when the Al content $x=0.056$, α can be calculated as $12.14 \times 10^{-4} \text{ eV/K}$ using Eq. (3), while β is determined as 1416.68 K according to Eq. (4). Similarly, for $\text{In}_x\text{Ga}_{1-x}\text{N}/\text{GaN}$ blue LEDs, the parameter x signifies the In component. When the In content $x=0.1$, α is $10.90 \times 10^{-4} \text{ eV/K}$ using Eq. (5), and β is determined as 1335.7 K using Eq.(6).

$$\alpha(\text{Al}_x\text{Ga}_{1-x}\text{N}) = x \cdot \alpha(\text{AlN}) + (1 - x) \cdot \alpha(\text{GaN}) \quad (3)$$

$$\alpha(\text{In}_x\text{Ga}_{1-x}\text{N}) = x \cdot \alpha(\text{InN}) + (1 - x) \cdot \alpha(\text{GaN}) \quad (5)$$

$$\beta(\text{Al}_x\text{Ga}_{1-x}\text{N}) = x \cdot \beta(\text{AlN}) + (1 - x) \cdot \beta(\text{GaN}) \quad (4)$$

$$\beta(\text{In}_x\text{Ga}_{1-x}\text{N}) = x \cdot \beta(\text{InN}) + (1 - x) \cdot \beta(\text{GaN}) \quad (6)$$

Table 3. Bandgap temperature coefficient in Varshni formula for III-nitride materials [17,18]

Bandgap temperature coefficients	AlN	GaN	InN
$\alpha(10^{-4} \text{ eV/K})$	17.99	11.8	2.87
$\beta(\text{K})$	1462	1414	631

Fig. 6 illustrates the temperature-dependent trend of the bandgap for violet LED and blue LED. As depicted in Fig. 6, the bandgap shows a decreasing tendency with increasing

temperatures.

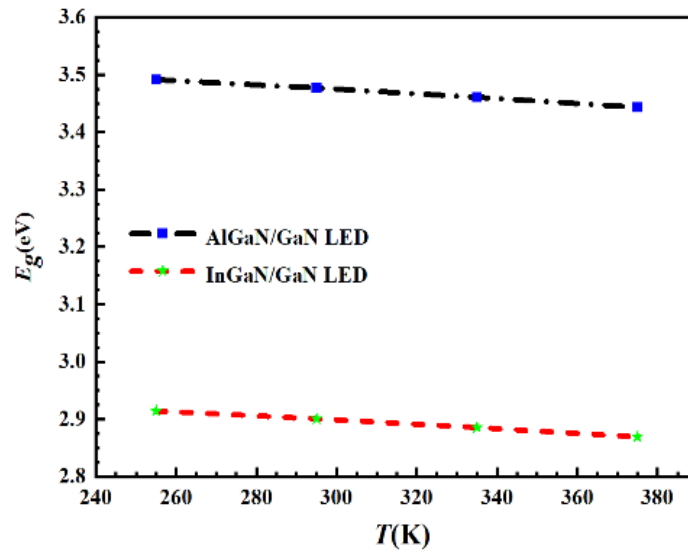


Fig. 6. The bandgap of violet LED and blue LED varies with increasing temperature (color online)

3.6. Electrical properties

The ideality factor n extracted from I-V curve, as a significant parameter for estimating the dominative recombination mechanisms of the LEDs. According to Shockley theory, the typical ideality factor range is 1-2, indicating the dominant recombination is either radiative recombination current or diffusion current. However, for GaN-based LEDs, the ideality factor n is much greater than 2, and is dominative due to the tunneling current instead of the thermal diffusion [19]. A higher ideality factor n indicates that not only affected by the carrier transmission process, but also the temperature during the higher current density injection. The I-V characteristics curve of the LED and the ideality factor n can be expressed as Eq. (7):

$$I = I_s \left[\exp\left(\frac{qV}{nkT}\right) - 1 \right] \quad (7)$$

Here I_s is the reverse saturation current, k is Boltzmann constant, q is the electron charge, and T is temperature.

At the temperature of 295 K, the I-V fitting curves for violet LED and blue LED are shown in Fig. 7 according to Eq. (7). The extracted results of ideality factor are presented in Table 4. From Table 4, one can see that the ideality factor of violet LED and blue LED both decrease with the increasing temperature, which is attributed to the carrier tunneling effect influenced by trapping phenomena [21,22] and are consistent with the Ref. [23,24]. Further analysis can be seen that during the studied temperature, the ideality factor for violet LED drops from 7.23 to 3.32, while blue

LED drops from 9.31 to 4.73, which has the similar tendency as in Ref. 23. Fig. 8 provides linearity fitting for the relationships between temperature and the ideality factor for violet LED and blue LED. It can be seen from Fig. 8 that the temperature factor of ideality factors of violet LED and blue LED are negative, and the temperature factor

of ideality factor of blue LED is $-0.03501/\text{K}$, while the temperature factor of ideality factor of violet LED is $-0.02988/\text{K}$, which indicates that the carrier recombination mechanisms are dominated by the tunneling recombination, higher charge fluctuation at the heterojunction interface [23].

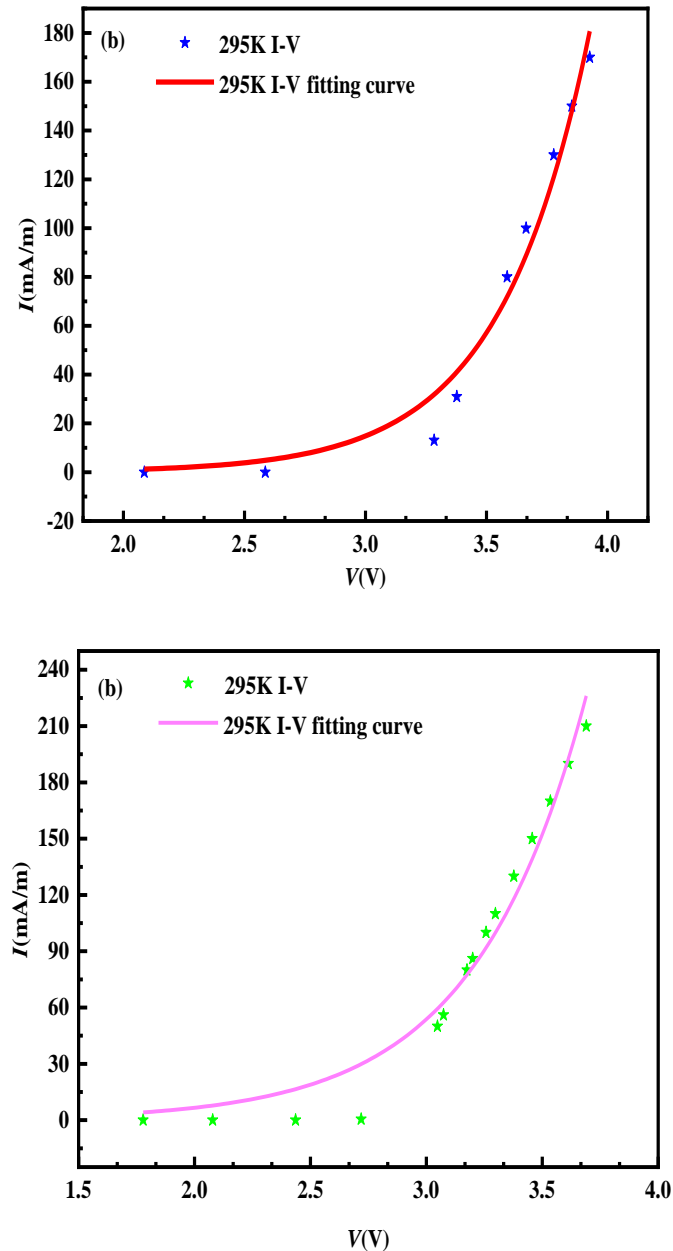


Fig. 7. Fitting curves of (a) violet LED and (b) blue LED at the temperature of 295 K (color online)

Table 4. Ideality factor of violet LED and blue LED at studied temperatures

LED	255 K	295 K	335 K	375 K
Violet LED	7.23	4.85	4.15	3.32
Blue LED	9.31	6.29	5.73	4.73

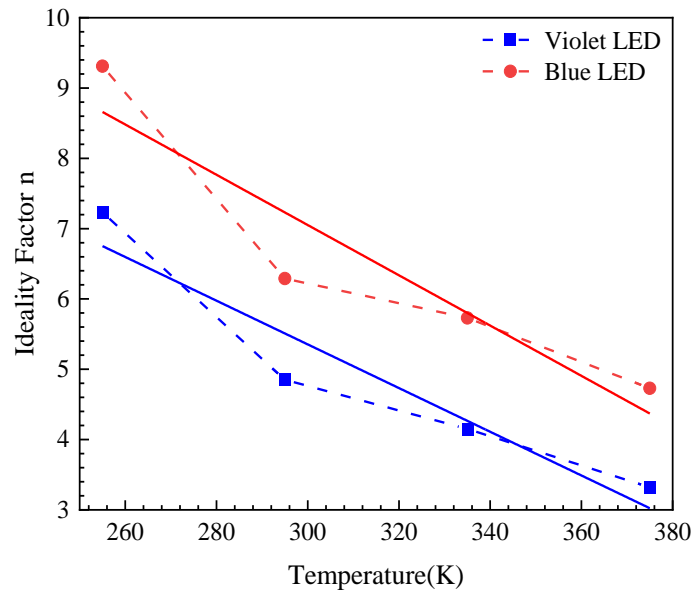


Fig. 8. Linearity fitting of ideality factors of (a) violet LED and (b) blue LED at the examined temperatures (color online)

4. Conclusions

In this study, APSYS software was utilized to investigate the relationships between the luminescence properties and electrical properties and temperature of violet LED and blue LED grown along the c-axis direction. The impact of bandgap, optical output power, quantum efficiency and electrical properties are investigated under the temperature range from 255K to 375K, and reveals a strong temperature-dependent between the luminescence properties and electrical properties and temperature. In addition, one can be concluded that temperature has a more sensitive effect on that of blue LED compared with violet LED.

Acknowledgments

Supported by Research and Practice Project on Comprehensive Reform of Graduate Education in Xi'an Shiyou University: A Preliminary Study on Breaking Through the Postgraduate Training Model with the Goal of "Stuck Neck": A Case Study of the Semiconductor Field (No.: 2023-X-YJG-024).

References

- [1] M. Usman, U. Mushtaq, D.-G. Zheng, D.-P. Han, N. Muhammad, *Materials Research Express* **6**(4), 04590 (2019).
- [2] K. J. Chen, O. Häberlen, A. Lidow, C. Tsai, T. Ueda, Y. Uemoto, Y.-F. Wu, *IEEE Transactions on Electron Device* **64**(3), 77 (2017).
- [3] H. Tao, Y. Xu, X. Huang, J.-Z. Chen, L. Pei, J. Zhang, J. G. Chen, Bin Liu, *IEEE Transactions on Electron Devices* **66**(1), 47 (2019).
- [4] Y. Yang, L. Zhang, T. Wei, Z. Yiping, *Journal of Display Technology* **11**(5), 45 (2015).
- [5] Liya Feng, Huimin Lu, Yifan Zhu, Yiyong Chen, Tongjun Yu, Jianping Wang, *Acta Physica Sinica* **72**(4), 299 (2023).
- [6] Kai Zhang, *Optical investigation on InGaN/GaN Multiple Quantum Wells* **02**, 1 (2016), (Doctoral dissertation of Shandong University).
- [7] Tong Liu, *Research on growth and photoelectric properties of AlInGaN Multi-Quantum Wells luminescent materials* **02**, 1 (2016), (Doctoral dissertation of Harbin Institute of Technology).
- [8] Shuanjun Lv, *Research on process and application of Indium doping barrier layers of InGaN/GaN MQWs* **03** (2011), (Doctoral dissertation of Xidian University)
- [9] Vikas Pendem, Pratim Kumar Saha, Shonal Chouksey, Swaroop Ganguly, Dipankar Saha, *Journal of Luminescence* **229**, 117703 (2021).
- [10] Yehui We, *Effect of growth temperature of well layers on optical properties of InGaN/GaN MQW-based LED* **6** (2020), (Doctoral dissertation of Shandong University).
- [11] Lida Su, *Quantum Well Structure of UV-LED Based on Group III Nitrides* **04** (2022), (Doctoral dissertation of Xidian

- University).
- [12] Wang Dang-Hui, Xu Sheng-Rui, Hao Yue, Xu Tian-Han, Zhang Jin-Cheng, Lin Zhi-Yu, Zhou Hao, Xue Xiao-Yong, *Chin. Phys. B* **22**(02), 028101 (2013).
- [13] Tao Hu, Youhua Zhu, Daishan Zhong, Meiyu Wang, Yi Li, *Semiconductor Technology* **48**(01), 18 (2023).
- [14] Yong Wang, Shengde Li, Zihan Wang, Jingcheng Xu, *Nonferrous Metal Materials and Engineering* **44**(03), 73 (2023).
- [15] Y. A. Yin, N. Wang, G. Fank, S. Li, *IEEE Transactions on Electron Devices* **61**(8), 284 (2014).
- [16] U. Ozgur, L. Huiyong, L. Xing, N. Xianfeng, H. Morkoç, *Proceedings of the IEEE* **98**(7), 1180 (2010).
- [17] I. V. Vainshtein, A. F. Zatspein, V. S. Kortov, *Physics of The Solid State* **41**(6), 90 (1999).
- [18] A. J. Fischer, W. Shan, J. J. Song, Y. C. Chang, R. Horning, B. Goldenberg, *Appl. Phys. Lett* **71**, 1981 (1997).
- [19] P. Perlin, M. Osinski, P. G. Eliseev, V. A. Smagley, M. Jian, M. Banas, P. Sartori, *Applied Physics Letter* **69**(12), 1680 (1996).
- [20] M. Missous, E. H. Rhoederick, *Electronics Letters* **22**(9), 47 (1986).
- [21] Shuping Shan, Y. Tongjun, Zhiliang Che, Guoyi Zhan, *Chinese Journal of Materials Research* **20**(02), 153 (2006).
- [22] Ma Ji-Zhao, Dong Ke-Xiu, Chen Dun-Jun, Lu Hai, Chen Peng, Zhang Rong and Zheng You-Dou, *Chinese Physics Letters* **30**(6), 068501(2013)
- [23] Yanjun Liao, Ding Li, Qi Guo, L. Yufeng, W. Haiming, H. Weiguo, *AIP Advances* **11**, 105214 (2021).
- [24] Di Zhu, Jiuru Xu, Ahmed N. Noemau, Jong Kyu Kim, E. Fred Schubert, Mary H. Crawford, Daniel D. Koleske, *Appl. Phys. Lett* **94**, 081113 (2009).

*Corresponding author: wdhyxp@outlook.com